Domain Confinement in Mesoscopic Epitaxial Cobalt Patches

Kamel Ounadjela, Michel Hehn, Ricardo Ferré

DOMAIN CONFINEMENT IN MESOSCOPIC EPITAXIAL COBALT PATCHES

Kamel Ounadjela, Michel Hehn and Ricardo Ferré

IPCMS, 23 rue du Loess, 67037 STRASBOURG Cédex, France

High resolution studies of nanostructured magnetic dots reveal a variety of intricate magnetic domain patterns controlled by details of the patterned geometry and of the magnetic history. Results are presented that show how the distribution and shape of the domains can be controlled. The high resolution studies were performed using the new and powerful technique of Magnetic Force Microscopy (MFM), which allows to discern features as small as 10 nm. A theoretical investigation of the domain structure has been performed and good agreement is shown between calculated and measured hysteresis loops as well as between calculated magnetic configurations and domain patterns observed by MFM.

INTRODUCTION

Advances in materials growth and characterization have, over the past ten years, made possible the investigation of basic physical processes in new 'artificial' materials. These materials are artificial in the sense that the geometry and composition are controlled during growth on micrometer and nanometer length scales. This results in macroscopic behavior that can be dramatically different from that of a material in its bulk form. Examples from the world of semiconducting superlattices are well known, but studies of high quality magnetic superlattices and microstructures have only recently begun. Tantalizing new possibilities have already appeared as in fact discussed not long ago in a special issue of Physics Today [1]. Much attention has been devoted to remarkable magnetic features such as oscillatory behavior of the exchange coupling [2], perpendicular magnetic anisotropy [3], giant magnetoresistance [4] and quantum size effect in magneto-optical properties observed in magnetic and metallic ultrathin films and related layered structures [5]. Those fundamental developments also made them of great interest from technological points of view in the area of communication devices and storage media.

One of the most stimulating extension of this research consist of investigating the properties arising from lower dimensional (lines, patches) and nanometer scaled magnetic structures. Such artificial magnetic structures are of interest due to their unique and unusual properties which are governed by their micromagnetic structure at nanometer length scales. To study static and dynamic magnetism of very small particles, say a few 10 to a few 100 nm, two approaches are possible. The first one consists in studying one single particle at a time with a very local technique like a SQUID loop surrounding the particle to be studied [6]. The second technique consists in performing an ensemble average measurement on an assembly of many identical particles [7]. While the first approach is mainly limited by technological and sensitivity considerations, the second one has been hampered by the difficulty of synthesizing a huge amount of perfectly identical particles. With the X-ray [8] and e-beam [9] techniques available today this limitation is largely overcome. An additional advantage of working with arrays is that by varying the period of the array, the magnitude of the interaction between the particles can be tuned : it was shown that the switching field is reduced for interacting permalloy particles formed by nanolithography techniques [10]. Magnetic order and reversal processes which have been extensively studied since the turn of the century have now to be reexamined for nanostructured materials.

The results on domain structure in submicron magnetic patches presented here exemplify current state-of-the-art in growth and imaging technologies. Equally important, these are the first reported results of periodic domains with magnetization perpendicular to the substrate in submicronic magnetic patches and they demonstrate the potential for precise control of micromagnetic behavior in patterned materials. Before discussing these results, the basics of domain formation are reviewed. A discussion then follows in which film thickness and pattern shape effects are examined.

DOMAIN FORMATION IN THIN FILMS

Exchange due to Pauli exclusion tends to align magnetic moments in a ferromagnet whereas interaction with crystalline fields via spin orbit coupling can lead to preferential orientation of the magnetic moments along particular directions. This behaviors are often described in terms of effective exchange and anisotropy fields acting on a position dependent magnetization vector. The concept of domain (volume where ail the magnetic moments are aligned) was originally introduced by Weiss [11] to explain why ferromagnetic materials can have zero average magnetization while still having a non-zero local magnetization. The essential idea is that the energy in a zero applied field can be minimized by changing the direction of the magnetization from one domain to the next one. The transition from one easy direction of magnetization to another between adjacent domains involves a rotation of the magnetization vector. The rotation occurs over a finite distance whose width is determined by a competition between exchange and anisotropy. The resulting magnetic structure is called a domain wall. When a magnetic field is applied, domains with the magnetization oriented along the applied field direction grow by displacement of the walls at the expense of domains with the magnetization oriented opposite to the field direction.

In three dimensional reality, numerous domain shapes exist. Under suitable conditions, magnetic domains in thin plates of some ferrimagnetic oxides have the shape of circular cylinders (bubble domains) or serpentine (stripe domains) with the magnetization perpendicular to the surface of the plate. A large amount of work performed in the 70's on bubble and stripe domains observed mainly in single crystals of orthoferrites, hexagonal ferrites and garnets was performed with the idea of using these surprisingly stable structures for storing and processing binary data in magnetic recording devices [12,13]. Typical bubble diameters were on the order of 10 μm, and do not allow for sufficiently dense packing of information to be competitive.

DOMAINS IN MESOSCOPIC FERROMAGNETS

The high quality epitaxially grown ferromagnetic *metallic* films now available have large saturation magnetizations and controllable anisotropies. This means that a thin Co film, for example, can be manufactured to support useful domain structures such as bubbles with diameters 100 to 1000 times smaller than in garnets. This is obviously exciting from the point of view of possible applications. Recently [14], we have studied thin hcp (0,0,0,1) Co films grown on Ru buffers. Strong perpendicular magneto-crystalline anisotropy, K, has been measured which makes the magnetization to switch from in-plane (Fig.1a) to out of plane (Fig.1c) as the film thickness increases.

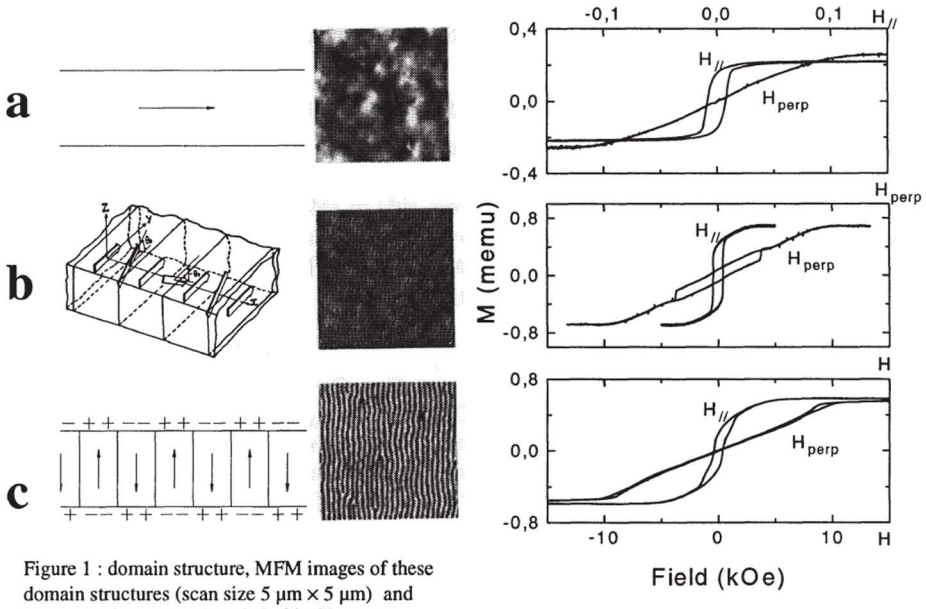

Figure 1 : domain structure, MFM images of these domain structures (scan size 5 μm × 5 μm) and magnetization curves in cobalt thin films as a function of thickness (a) 10 nm (b) 25 nm and (c) 100 nm.

This was predicted by Kittel [15] on energetic arguments (competition between wall and magneto-static energy) and the predicted value of the film thickness d for which the magnetization turns from in plane to out of plane was calculated to be: [15]

$$d_1 \approx 6.8\sigma_w \left(\frac{M_s}{K}\right)^2 \qquad (1)$$

where M_S is the saturation magnetization and σ_w is the wall energy density. When this condition is applied to hcp cobalt films, the crossover is predicted to occur at about 30 nm [14]. The only way for a thicker film with out of plane magnetization to lower its energy is then to split up into small domains with up and down magnetization as shown in Fig. 1c. We have also identified a continuous reorientation of the magnetization in thin epitaxial cobalt films from fully in plane (Fig. 1a) to fully out of plane (Fig. 1c) for thicknesses comprised between 10 nm and 50 nm similarly to previous works [15]. This occurs through a magnetization configuration with in-plane and out-of-plane components (Fig. 1b) [14,16]. The observed domain patterns arise from the up and down components of the perpendicular magnetization. In all these cases, the patterns are stabilized by competing interactions leading to periodic variations of the order parameter [17].

Observing domains on nanometer length scales

The opportunity for new physical studies appears when domain patterns are induced in magnetic structures constructed with dimensions on the order of few hundred of nanometers or less. In Co, the characteristic nanoscopic length scales as exchange

length on the order of 10nm ($\sqrt{A}/M_S$), the width of a domain wall around 20nm ($\pi\sqrt{A/K}$ =14nm for a Bloch wall, A being the exchange stiffness) and mesoscopic dimensions as domain width becomes then comparable to the sample dimensions. The lateral dimension of each patch is 500nm, the thickness varies from 25nm to 150nm. Up to ten domains were counted from side to side of the patch implying that the domain walls are therefore separated by a distance involving around 250 atoms. Effects of the boundaries become then apparent and the domain geometry is strongly dependent on the aspect ratio of the magnetic patches.

The samples are 5 x 5 mm^2 square array of square dots with 0.5 µm lateral dimension and 1µm array periodicity as shown in Fig.2. They were fabricated on Ru(5 nm)/Co(t_{Co})/Ru(20 nm)/Al2O3(1,1,-2,0) films with t_{Co} varying from 10 to 150 nm using X-ray lithography and ion beam etching. The films were prepared by electron beam evaporation. The crystallographic structure of the films was studied using different *in situ and ex situ* techniques reported elsewhere [14,18] which reflect the high crystallinity of the film and reveal a very good hep (0,0,0,1) phase for the cobalt films grown at 400°C. Moreover, additional NMR experiments have indicated a reduced diffusion over only four atomic layers at the interface between the cobalt and ruthenium [14]. Cobalt films were patterned using a soft technique developed earlier to avoid deteriorating fragile multilayered samples. The patterning process begins with the creation of holes in an high sensitivity resist using X-ray lithography followed by an aluminium lift off process. In this way, during the ion beam etching, the aluminium mask is used to protect the future cobalt dots while the other part of the film is etched.

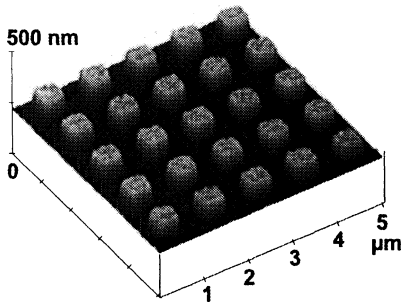

Figure 2 : Oblique view of a 25 nm thick Co dot array obtained with an Atomic Force Microscope. The dot lateral size is 0.5 µm and the lattice periodicity is 1 µm. The edges are straight with nearly vertical profile and the surface of the dots have retained the smoothness already observed on the as grown films. This quality of patteming is rnaintained for up to 150 nm thick Co films.

Details of this technique have been summarized elsewhere [8]. An example of etched array is given on Fig. 2 for a 25 nm thick cobalt. The edges are straight with nearly vertical profile and the dots surface retain the smoothness already observed on the as grown films. This quality of patterning is kept up to 150 nm

thick cobalt films.

Global magnetization measurements were performed for all samples at room temperature in an Alternating Gradient Force Magnetometer (AGFM) with the field applied perpendicular and parallel to the film plane and local magnetization measurements were performed using Magnetic Force Microscopy (MFM). With MFM, the resolution is solely limited by the distance at which the tip is scanned above the surface and the tip radius, typically 10 nm. The tip cannot approach the surface too closely because short-range topography signals would interfere with the long-range magnetic information. A Nanoscope III, equipped with a CoCr coated Si tip magnetized along the tip axis, was used in the vibrating-lift mode developed by Digital Instruments. The detected signal (frequency shift of the vibrating cantilever), is proportional to the second derivative of the local field, and therefore this technique provides a good signal to noise ratio. For domain sizes under consideration here we have shown that MFM contrasts can be identified unequivocally with "up" and "down" oriented domains [14].

Effects of microscopic structure on domain formation

Quantitative information on the occurrence of domains are obtained from magnetization curves. This is exemplified in Fig. 3 and 4 which reveal similarities and differences in magnetic behaviour of arrays and films. First of all similarities appears in the shape of the magnetization curves (with the field applied perpendicular (Fig. 3a) and parallel (Fig. 4a) to the substrate) shown for a 100 nm thick film and array. Both curves in the perpendicular orientation of the external field (Fig. 3a) appear like a signature of perpendicular magnetized multidomain structure [19-21]. As the perpendicular applied field is greater than the saturation field H_s, the slope of the curve seems to vanish. But a close examination of Fig. 3a reveals that the magnetization slightly increases as the field is further increased. This fact is attributed to the disappearance of domain walls which are still present in the magnetic « saturated » state in the form of closed walls surrounding domains with vanishingly small dimensions (vestigial domains). As the applied field is decreased, the diameter of these vestigial domains increases. Nucleation takes place as the applied field is equal to H_n, the nucleation field. At this field, the vestigial bubble domain structure is submitted to an elliptic instability predicted by Thiele [20]. The kink that appears after saturation when the field is decreased is attributed to the run out into stripe-like domains. As the field is further reduced, the diameter of the stripe-like domain grows by wall motion inducing a quasi linear variation of the magnetization with the external field [19-21]. The transition from bright to dark bubbles proceeds continuously in a wall motion type of procedure as described elsewhere [14]. When the field is along the film plane (Fig. 4a), the magnetization curve is characteristic of a Stoner-Wolfarth like coherent magnetization rotation. The quadratic curvature of the loop and the remanence at zero field confirm the presence of magnetic stripe domains from the contribution of the magnetic walls. Differences on the major magnetic parameters, the saturation and nucleation fields, shown in Fig.3b and 4b as a function of the film thickness are clearly induced by the lateral size reduction of the films.

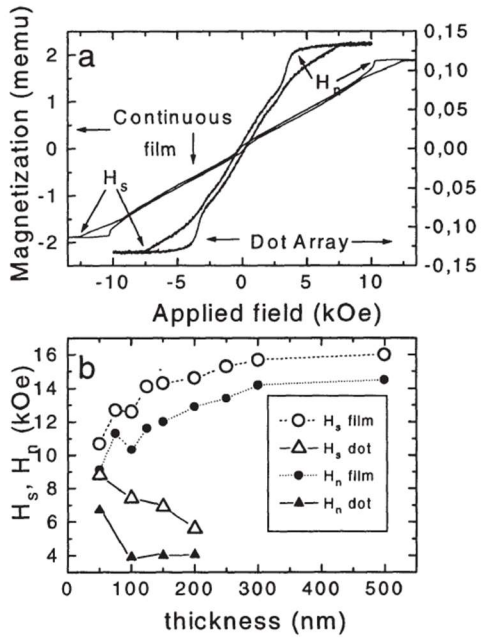

Figure 3 : (a) Perpendicular magnetization curves for a 100 nm thick film and dot array (b) Evolution of the nucleation (H_n) and saturation field (H_S) as a function of film thickness for films and dot arrays.

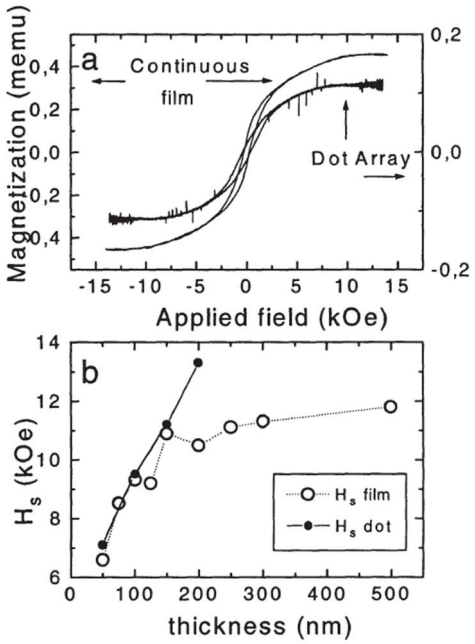

Figure 4 : (a) Parallel magnetization curves for a 100 nm thick film and dot array (b) evolution of the saturation field (H_S) as a function of film thickness for films and dot arrays.

This is easy to understand by considering the energies involved in the formation and collapse of perpendicular domains. In both the film and the array, a perpendicular magnetocrystalline anisotropy is present that tends to align the magnetization out-of-plane. The anisotropy defines the direction of the magnetization within the domains and together with exchange determines the energy involved in creating domain walls, but does not otherwise influence the energy of the configuration. Monodomain perpendicular orientation however is opposed by demagnetizing fields determined by the shape of the sample and the system has a natural tendency to split up into smaller domain with up and down magnetization in order to reduce the magnitude of the demagnetizing field experienced by the local magnetization. The domain structure disappears as the external magnetic field is increased beyond the saturation field. The demagnetizing field for a rectangular block is approximately given by

$$H_d = -8\, M_s \sin^{-1}(1/(1+r)) \qquad (2)$$

where r the height to width ratio (aspect ratio). This gives a maximum reduction of 37% of the demagnetizing field (in the case of a single domain structure) from that of a continuous film if the aspect ratio of the rectangular block is 0.2. The reduction in the nucleation and saturation fields for the dot array is clearly seen in Fig. 3b because of the large size of the domains (100 nm) which is comparable to the dot size. Similar arguments can be given to explain the increase of the parallel saturation field for the dots with respect to the continuous films.

Since by MFM we do not have access to high magnetic field, we rely on probing the sample through well defined magnetic history. Along this idea, we have performed both magnetization and demagnetization experiments in direction either perpendicular or parallel to the plane of the film. During the demagnetization, (quoted PaDm and PeDm for Parallel and Perpendicular Demagnetization respectively in Fig. 5) the field is swept from positive to negative values while reducing simultaneously the maximum applied field and so the area of the hysteresis loop. In the case of perpendicular magnetization (quoted PeRm for Perpendicular Remanence in Fig. 5), the magnetization is brought to saturation and the field is turned off leading the system to reach its remanent state. All the MFM images shown in this paper were taken at zero field.

Similarly to what bas been observed in the cobalt films (Fig. 5a), the formation of bubble and stripe domains is possible in the magnetic patch array but in a manner very sensitive to the direction of the applied demagnetizing field. This is indeed indicated by our results on the 50 nm (Fig. 5b PaDm) and the 150 nm (Fig. 5c PaDm) thick Co patches where stripe patterns appear after an external parallel demagnetization. A straight stripe domain pattern is observed. In the case of the 50 nm thick sample, the stripes direction is given by the magnetic field component in plane prior to relaxation. The tendency of the domains to avoid the edges of the dot and to increase the surface of the domain wall is stressed in the case of the 50 nm thick dot (fig 5b PaDm). These

peculiarities clearly appear as a results of the geometrical constrains and will be analysed in the next section.

Bubble domains appear in the remanent state after perpendicular saturation as shown in Fig. 5 (PeRm). The domain structure observed in a 50 nm thick cobalt dot array consists of a metastable network of bubbles which is very similar to the domain array found in the thick continuous film Fig.5a PeRm. At 150 nm, however, circular bubbles are nucleated at the center of the dot where the effective field is lowest and do not grow bigger due to the repulsive interactions with the edges. In comparison with Fig.5b PeRm, now the available space within each patch is just sufficient to accomodate one single bubble as shown in Fig.5c PeRm.

Shape effects - geometrical control of domain patterns
Two effects of patterning on domain formation can be distinguished: the effect of patch height and the effect of patch shape. Patch height determines domain size in much the same way as film thickness does. If the domain size is much smaller than the lateral dimension of the patch, one expects identical behavior for a continuous film and a magnetic patch array since the average stray demagnetizing fields outside a multidomain patch are very small. This means that the magnetostatic energy at any point inside a patch is primarily determined by nearby domains within the patch.

This can be verified by comparing domain size as a function of patch height to_domain size as a function of film thickness. Measured values for the diameter and stripe period show a functional power law behavior with exponent 0.5 as expected from theoretical predictions for magnetic films [15,21]. The dependences on patch height and film thickness are the same, although the stripe data appears to deviate from the film behavior for the thickest patch investigated. At this thickness, the domain size is close to the lateral dot size and dipolar stray fields from the edges may significantly affect the domain pattern and size.

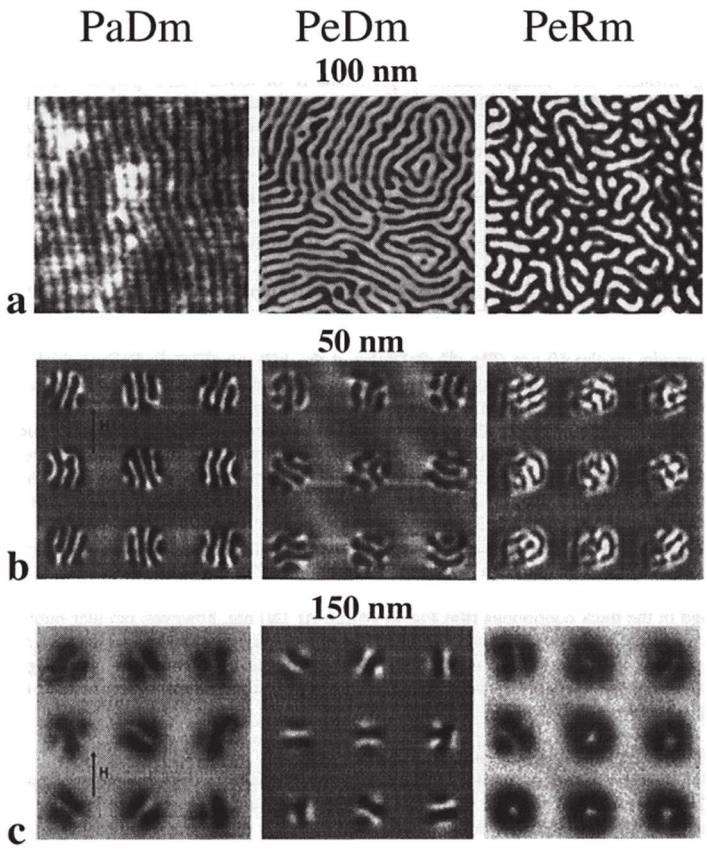

Figure *5* : MFM images obtained after parallel demagnetization (PaDm), perpendicular demagnetization (PeDm) and perpendicular saturation (PeRm) for a 100 nm thick film, *50* nm and 150 nm thick dot array (scan size 3 µm x 3 µm).

A simple argument can be given for the relation between film thickness and stripe domain period. The formation of a stripe pattern depends on reducing the magnetostatic energy at a cost of creating domain walls across the thickness of the film. Defining the lateral size of a domain in a periodic stripe structure as d and the film thickness as t, then the magneto-static energy is proportional to: $M_S^2 d$ [15]. If the energy per unit area of a domain wall is σ_w, and with 1/d domain walls per length along the film, then the energy cost of creating a domain in the film is $\sigma_w t/d$. The value of d that minimizes the sum of these two energies depends on $t^{1/2}$. One can also argue for a similar dependence of bubble domain diameter on film thickness.

Shape effects in the patch array dominate the orientation of domains in the patches and distinguish patterned array behavior from continuous film behavior. Finite size effects on the domain formation appear at ail thicknesses and is particularly interesting when domain width is comparable to the lateral extension of the dot. Figure 5c show the domain configuration in dots patterned from a 150 nm thick cobalt layer. For this thickness the expected stripe width in a continuous film is about 120 nm [14]. The remanent state after perpendicular magnetization in the dots is a predominantly single bubble configuration (Fig. 5c PeRm) although the precision of the MFM experiment

cannot exclude the presence of domains or "flower" states (slight canting of the magnetic moments) at the dot borders. The bubble locates in the center of the dot where the demagnetizing field is the smallest and did not grow bigger due to the repulsion of the edges.

Some arguments can be given to explain the formation of domains during in-plane demagnetization. In the range of thicknesses above 50 nm, the magnetization curves are characteristic of perpendicularly oriented magnetic domains. As the dot is submitted to a large enough in-plane magnetic field, one expects ail magnetic moments to align along the field direction. When the field is decreased, and while the main component of the magnetization remains in-plane, vortices start to form at the corners of the dots in order to reduce the in-plane demagnetizing field. The mechanism is similar to the one described for permalloy particles with in-plane magnetization [22,23] where the vortices are shown to move towards the center of the dot as the field is further decreased. In order to minimize the exchange energy, the magnetization at the center of the vortex is perpendicular to the surface. During the field decrease the magnetization rotates coherently out-of-plane resulting in a magnetization perpendicular to the film with regions (where vortices were created, that is mostly at corners) with opposite magnetization.

When the bubble diameter is comparable to the lateral dimensions of the dot (as for 150 nm thick dot array), only two bubbles nucleate at opposite corners in order to minimize their repulsive interaction which coalesce to form dumb-bell domains (Figs.5c PaRm). For symmetry reasons, when the field is applied along the side of a dot, the dumb bells will be aligned either along one diagonal or the other as can be shown from figure 5c PaRm. When the bubble diameter is small compared to the lateral dimensions of the dot (as for the 50 nm thick dot array), the bubble nucleated at the edge remains pinned on it but can run out into stripes (Figs. 5b PaRm) if there is enough space to accommodate more than one domain.

What distinguishes the 25 nm thick dots from the thicker ones is the magnetization curves, characteristic of mostly in-plane magnetization with small alternately up and down perpendicular components, as reported in reference [24] and shown in Fig.1b for hep cobalt films. The nucleation process remains similar to the one explained previously but the main component of the magnetization is now in-plane. The particular domain structure must be analyzed in terms of in-plane and out-of-plane components of magnetization. First, the in-plane magnetostatic energy is reduced for in-plane magnetic moments parallel to the edges of the dots which results in circular domain structure as shown in Fig. 6a. This implies that a singularity occurs at the center of the dot where the in-plane magnetization reorients fully perpendicular to form a so-called vortex structure. Secondly, in order to reduce the perpendicular magnetostatic energy, the small perpendicular component of magnetization adopts a concentric magnetic domain pattern in agreement with the weak contrast observed by MFM (Fig. 6a).

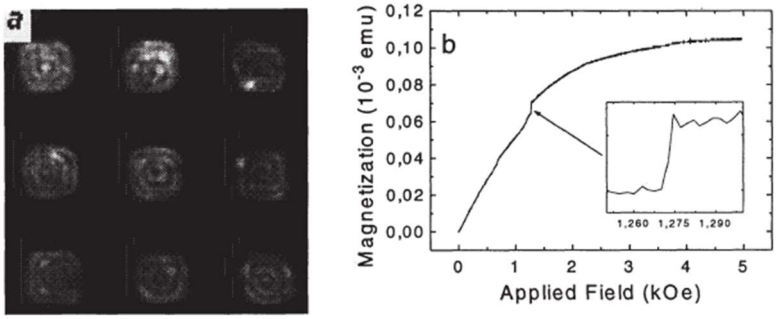

Figure 6 : (a) MFM image for a 25 nm thick dot array obtained after parallel demagnetization (scan size 3 µm x 3 µm) and (b) First perpendicular magnetization curve for the 25 nm thick Co dot array. The inset shows a zoom of the region where the jump occurs and gives evidence of the field transition within 2 Oe.

How domain confinement proceeds is particularly interesting to investigate in the 25 nm thick Co dot array. The curve of the first perpendicular magnetization (Fig. 6b), taken after the sample bas undergone in-plane demagnetization, displays one pronounced jump of the magnetization which occurs within a field interval of 2 Oe. Since the dipolar interaction between dots is so weak that no collective behavior can be invoked to explain this phenomenon, the observation of the simultaneous switching of millions of dots necessarily implies that the collapse field is mostly sensitive to local parameters like thickness and quality of the material, in principle identical over the whole sample surface. We attribute this singularity, which corresponds to about 6% of the magnetization at saturation, to the collapse of central domains, less sensitive to dots shape and edges of dots with central magnetization oriented antiparallel to the field direction (about half of the dots of the array). Close examination of the magnetization curve (Fig. 6b) reveals at least two more, although weaker, jumps at lower field (reproducible under identical conditions) which can be attributed to the initial collapse of part of the outer rings. Such a distribution of jumps may result because the height of one jump is proportional to both, the size of the domain to be reversed and to the number of dots with the same configuration. Not surprisingly, after the dots have become single domain, further increase of the field is necessary to overcome the strong demagnetizing field near the bottom and the top of the dots and completely align the moments along the field direction.

To further improve the interpretation of these experimental results, we have undertaken 3D-Micromagnetic calculations of domain configurations in submicronic cobalt dots. Details of the technique are given in Ref. 25. Good agreement is shown between the calculated and measured hysteresis loops as well as between the calculated and experimental domain patterns discussed in this paper.

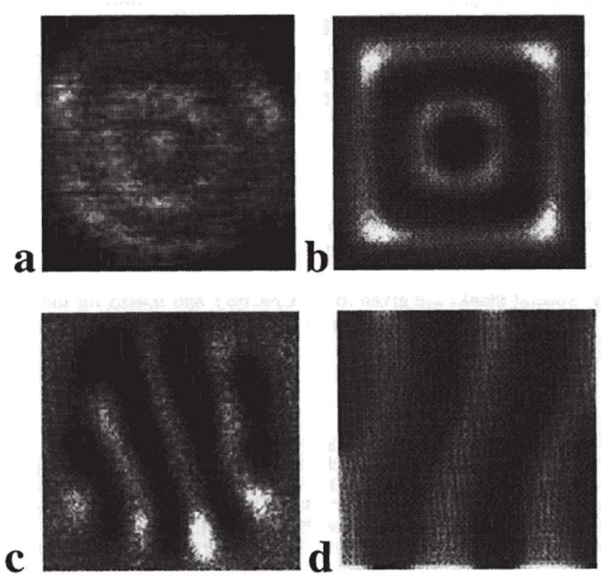

Figure 7 : Experimental MFM images obtained for a (a) 25 nm (c) 50 nm thick dot (scan size 0.5 μm x 0.5 μm) and respectively their theoretical simulations (b) 25 nm and (d) 50 nm (size 0.2 μm x 0.2 μm).

To show the excellent agreement between experiments and theory, two examples are shown in Fig. 7 for the 25 nm and 50 nm thick cobalt dots in the case of in-plane demagnetization. For the 25 nm thick cobalt dot, the appearance of a radially modulated vortex structure at zero field bas been found theoretically (Fig. 7b) and can be well compared to the experimental data (Fig. 7a). The domain wall configuration obtained for this system presents a Néel type wall at both surfaces of the dot whilst the inner part of the wall is of Bloch type [25]. The mean size of the wall is found to be 23 nm, on the order of the Bloch wall size. For the 50 nm thick cobalt dot, the twiggled stripe domain structure observed experimentally (Fig. 7c) is found on the calculated magnetic patterned structure (Fig. 7d) and is attributed to the fact that at nucleation, oscillations in perpendicular magnetization are of opposite sign at the two borders and the only way for the system to overcome this "frustrating" situation is to form "twiggled" perpendicular domains. All these results have been discussed in details by Ferré et al in Ref. 25.

CONCLUSION

In summary, we have shown that two length scales determine the magnetic domain structures and magnetic domain reversal processes in cobalt dot arrays. One length scale is set by the geometry of the dots, the other one is imposed by the size of a domain wall separating two adjacent domains. Domain configurations such as concentric rings and spirals have been stabilized, which drastically influence the magnetization reversal process. When starting from a concentric rings configuration, clear jumps are observed in the first magnetization curve of an array which are clearly linked to specific domain annihilation processes. Interestingly, the micromagnetic

calculation agrees well with the experimental observation of the domain structure which suggest that the domain confinement in the mesoscopic array of cobalt dots are related to classical phenomenon.

ACKNOWLEDGEMENTS

The authors would like to thank Hugo van den Berg, J.P. Bucher, C. Chappert, F. Rousseaux, Robert Stamps and Philip Wigen for fruitful discussions and Frank Carcenac, Dominique Decanini and F. Rousseaux for their technical support in X-ray lithography. Special thanks are given to the CNCPST and IDRIS for the use of parallel computing facilities. This work was partly supported by the European Human Capital and Mobility program.

REFERENCES

[1] Physics Today, Special issue: magnetoelectronics 48 (1995).
[2] S.S. Parkin, N. More, and K. P. Roche, Oscillations in exchange coupling and magnetoresistance in metallic superlattice structures: Co/Ru, Co/Cr and Fe/Cr, Phys. Rev. Lett. 64, 2304 (1990).
[3] C. Chappert, K. LeDang, P. Beauvillain, H. Hurdequint and J.P. Renard, Ferromagnetic resonance studies of very thin cobalt films on a gold substrate, Phys. Rev. B 34, 3192 (1986).
[4] M. Baibich *et al,* Giant magnetoresistance of (001) Fe/ (001) Cr magnetic superlattices, Phys. Rev. Lett., 61, 2472 (1988).
[5] Y. Suzuki, T. Katayama, S. Yoshida, K. Tanaka, and K. Sato, New magneto-optical transition in ultrathin Fe (100) films, Phys. Rev. Lett., 68, 3355 (1992).
[6] W. Wernsdorfer *et al,* DC-SQUID magnetization measurements of single magnetic particles, J. Mag. Mag. Mat. 145, 33 (1995).
[7] A. D. Kent, S. von Molnar, S. Gider and D. D. Awschalom, Properties and measurement of scanning tunneling microscope fabricated ferromagnetic particle arrays (invited), J. Appl. Phys. 76, 6656 (1994).
[8] F. Rousseaux *et al,* Study of large area high density magnetic dot arrays fabricated using synchrotron radiation based x-ray lithography, IEPB95 Proc., J. Vac. Sei. Technol. B 13, 2787 (1995).
[9] R. M. H. New, R. F. W. Pease and R. L. White, Submicron patteming of thin cobalt films for magnetic storage, J. Vac. Sei. Technol. B 12, 3196 (1994).
[10] G. A. Gibson and S. Schultz, Magnetic force microscope study of the micromagnetics of submicrometer magnetic particles, J. Appl. Phys. 73, 4516 (1993) and refs therein.
[11] P. Weiss, L'hypothèse du champ moléculaire et la propriété ferromagnétique, J. Phys. (Paris) [4] 6,661 (1907).
[12] A. H. Eschenfelder, *Magnetic Bubble Technology,* Eds (Springer, Berlin, 1980). [13] A.H. Bobeck and E. Della Torre, *Magnetic Bubbles,* Eds (E.P. Wohlfarth, 1975).

[14] M. Hehn, S. Padovani, K. Ounadjela, J.P. Bucher, Nanoscale magnetic domain structures in epitaxial cobalt films, Phys. Rev. B, 54 (August 1996) and references therein.
[15] C. Kittel, Theory of the structure of ferromagnetic domains in films and small particles, Phys. Rev. 70, 965 (1946).
[16] K. Krishnan, Y. Honda, Y. Hirayama and M. Futamoto, Microstructure and epitaxy of c-axis oriented single crystal cobalt films grown on rigid underlayers, Appl. Phys. Lett. 64, 1499 (1994); D. Donnet, K. Krishnan, and Y. Yajima, Domain structures in epitaxially grown cobalt thin films, J. Phys. D, 28, 1942 (1995).
[17] M. Seul, and D. Andelman, Domain shapes and patterns : the phenomenology of modulated phases, Science, 267,476 (1995) and refs. therein.
[18] M. Hehn, K. Cherifi-Khodjaoui, K. Ounadjela, J.P. Bucher and J. Arabski, Engineering magnetic responses in hep cobalt thin films, J. Mag. Mag. Mat., in press.
[19] J.A. Cape and G.W. Lehman, Magnetic domain structures in thin uniaxial plates with perpendicular easy axis, J. Appl. Phys. 42, 5732 (1971).
[20] A.A. Thiele, The energy and general translation force of cylindrical magnetic domains, the Bell Syst. Tech. J. 50, 711 (1971).
[21] C. Kooy and U. Enz, Experimental and theoretical study of the domain configuration in thin layers of BaFe12O19, Philips Res. Rep. **15,** 7 (1960).
[22] D. R. Fredkin, T. R. Koehler, J.F. Smyth and S. Schultz, Magnetization reversai in permalloy particles : micromagnetic computations, J. Appl. Phys. **69,** 5276 (1991).
[23] T. R. Koehler and D. R. Fredkin, Micromagnetic modeling of permalloy particles : thickness effects, IEEE Trans. Mag. **27,** 4763 (1991).
[24] M. Hehn, **K.** Ounadjela, J.P. Bucher, F. Rousseaux, D. Decanini, B. Bartenlian, C. Chappert, Nanoscale magnetic domains in mesoscopic magnets, Science, **272,** 1782 (1996).
[25] R. Ferré, M. Hehn and K. Ounadjela, Nanoscale magnetic domains in mesoscopic dots : micromagnetic investigation of magnetization processes, J. Mag. Mag. Mat., in press.